Available online at www.sciencedirect.com
ScienceDirect
Radiation Physics and Chemistry 75 (2006) 1582–1585
Radiation Physics and Chemistry
www.elsevier.com/locate/radphyschem

Atomic cluster calculation of the X-ray near-edge absorption of copper

C. Witte, C.T. Chantler*, E.C. Cosgriff, C.Q. Tran

School of Physics, University of Melbourne, Victoria 3010, Australia

Accepted 9 July 2005

Abstract

The finite difference method for near-edge structure is used to calculate X-ray absorption near-edge structure (XANES) spectra. We extend the range of calculation for copper above the K-shell threshold and compare the results with recent experimental data in the X-ray absorption fine structure (XAFS) region. Qualitatively the calculation predicts the location of the peaks but fails to accurately describe relative amplitudes.

PACS: 78.70.Dm; 61.10.Ht; 78.20.Bh; 32.80.Fb

Keywords: XAFS; XANES; Copper

1. Background

X-ray absorption fine structure (XAFS) contains detailed information about the local structure, in particular about nearest neighbour distances, coordination numbers, fluctuations in bond distances, electronic structure and vibrational structure, providing a unique thumb print of the material being investigated. An accurate theoretical model validated by precise experiments is needed to utilise this field to its full potential. Significant progress has been made (Chantler, 1994), but discrepancies exist between theoretical approaches of up to 200% for numerous elements in the 1–3 keV X-ray energies (Chantler, 2000), and until recently experimental inaccuracies have made it impossible to differentiate between them. Recent experimental work using the X-ray extended range technique (XERT) has improved accuracies to a level of 0.27–0.4% (Tran et al., 2005) prompting renewed efforts to improve theory.

Qualitatively XAFS can be explained by many-body effects such as shake-up and shake-down, inelastic scattering and multiple scattering but accurate ab initio calculations that include these effects have been missing or are severely limited.

Cluster methods can reproduce solid state effects but most use the muffin-tin potential. In this approximation the potential in a sphere of radius r surrounding the atom is expanded in spherical harmonics. In the interstitial region between atoms the potential is assumed constant. The size of the muffin tins is then a free parameter varied to obtain the best match. Often overlapping spheres produce the best results. This is a questionable formal assumption of the methods and can hide structural or electronic information. The presence of a free parameter to match experimental data questions the significance and sensitivity of this assumption.

Joly (2001) proposed using the finite difference method (FDM) to calculate the potential in the

*Corresponding author.
E-mail address: chantler@physics.unimelb.edu.au (C.T. Chantler).

0969-806X/$ - see front matter © 2006 Elsevier Ltd. All rights reserved.
doi:10.1016/j.radphyschem.2005.07.018

interstitial region. This cluster calculation makes no assumptions about the shape of the potential. Joly implemented this finite difference method for near-edge structure (FDMNES). Space is partitioned into the atomic core region, the interstitial region and the outer sphere. The potential is calculated using the local density approximation. The FDM per se is only used in the interstitial region. In the atomic core the potential is assumed to be spherically symmetric and expanded in spherical harmonics similarly to the approach of the muffin-tin potential. This region is generally smaller than that typically used in the muffin-tin approach.

In the interstitial region the FDM is used and Schrödinger's equation is discretised, with the Laplacian being replaced by a fourth-order polynomial and solved on a discrete lattice. In the outer sphere, the solution is again assumed to be spherically symmetric and is expanded in Neumann and Bessel (or Hankel) functions. The three regions are then solved by requiring continuity across the boundaries (Joly, 1996, 2001). This method was proposed for XANES calculation. Here we explore extending these results into the XAFS region for the K-shell of copper and compare these with experimental results.

2. Multipole expansion convergence and comparison with a muffin-tin potential

The FDMNES program can perform calculation in the multipole expansion in dipole, quadrupole or octupole order. A comparison was performed for a 3 Å copper cluster in the dipole, quadrupole and octupole expansion. Fig. 1 shows that the higher-order expansions make little difference to the results. This is expected as the K-shell ionisation of copper is dominated by the dipole term: i.e. it is a semi-classically allowed $\Delta l = 1$ transition.

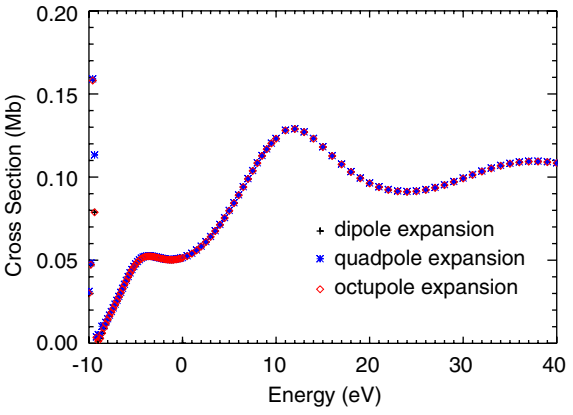

Fig. 1. Calculations in the dipole, quadrupole and octupole expansion for the K edge in copper. The inclusion of higher-order multipoles makes little difference as the K-shell ionisation of copper is dominated by the dipole term.

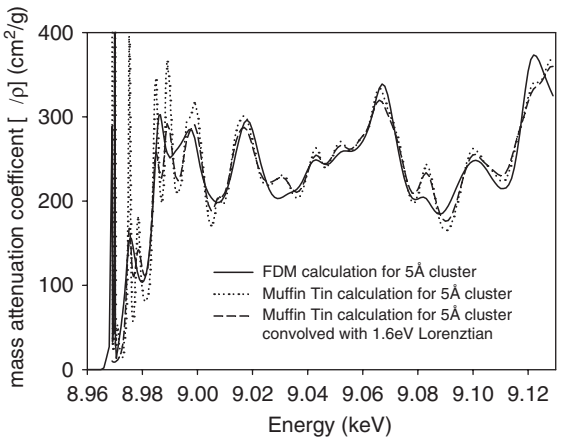

Fig. 2. Calculations for a 5 Å copper cluster using the FDM and the muffin-tin potential. This muffin-tin calculation is much more sharply peaked and does not produces the same peak locations.

The FDMNES program can also compute an implementation of the muffin-tin approximation, allowing a comparison to be made between the two methods. Fig. 2 demonstrates that this muffin-tin implementation yields much more sharply peaked oscillations than the corresponding FDM approach. The two methods also predict different peak locations.

We do not conclude that this is a failure of the muffin-tin approach. The symmetry of the muffin-tin model should be quite appropriate for the purposes of metallic (infinite) Mo, and there are several different muffin-tin approaches; but the constancy of the intervening potential may be an issue.

3. Computational scaling and convergence

One of the major stated limitations of the FDM is that it is limited to energies just above the threshold. The maximum angular momentum used to connect the interstitial region to the outer sphere is given by

$$kr = \sqrt{l_{\max}(l_{\max}+1)}, \quad (1)$$

where k is the photo-electron wave vector and r is the cluster radius. This imposes practical limits on the possible calculations. As the energy above the threshold increases the angular momentum basis set increases almost linearly. Calculations in the range 80–90 eV take more than twice as long as calculations for the region 0–10 eV above the threshold. It is also necessary to increase the cluster radius to prevent numerical instabilities and ensure sufficient spherical harmonics to

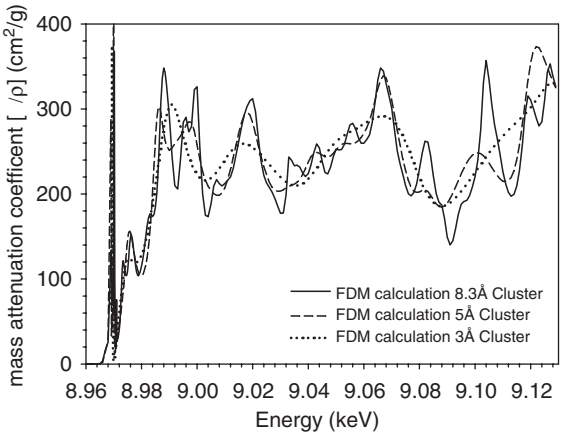

Fig. 3. Comparison of the FDMNES calculation for clusters of 3, 5 and 8.3 Å. Convergence is reached for a 8.3 Å cluster. The larger cluster size reveals finer oscillations (in different locations from the muffin-tin prediction) but the smoothed or broadened spectrum is consistent.

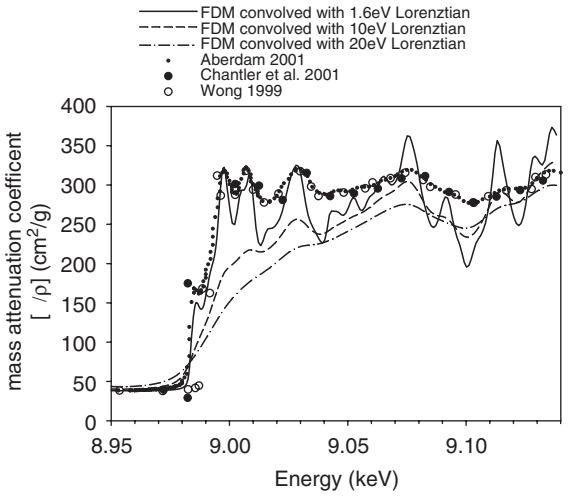

Fig. 4. Details of the near-edge oscillations showing a comparison with the theoretical predictions from FDMNES. Calculations for a 8.3 Å copper cluster convolved with 1.6, 10 and 20 eV Lorentzians. The relative experimental data of Aberdam (2001) and Wong (1999) was accordingly scaled to match the absolute measurements Chantler et al. (2001). Given the scaling, experiments are in accord.

describe the outgoing wave correctly as the energy is increasing. The scaling with cluster size is greater than n and is more like n^2, where n is the number of atoms in the cluster. This has unfortunately limited the applicability of FDMNES to calculations near the edge and Rehr and Albers (2000) has therefore stated that, while FDMNES is a beautiful technique, it is limited to XANES and does not apply to XAFS.

Finer oscillations are revealed in the spectrum as the cluster size increases (Fig. 3), but if a moderate broadening is assumed the results are consistent. As reported in Joly (2001), convergence is reached for a 8.3 Å cluster. While bound–bound transitions are forbidden in this particular experiment (all the available orbital energies are below the Fermi level and are occupied), the FDMNES program allows this level to be set (e.g. if an ionised state were being investigated). This is the 'pre-edge peak' on the figure which is corrected (removed) before further analysis.

4. Broadening

The hole width is not included in the FDMNES code and must be taken into account after the calculation. Theoretical results for the hole width are in the range 1.43–1.77 eV (Scofield, 1974; McGuire, 1970). To allow for this, we convolve an 8.3 Å calculation with a 1.6 eV Lorentzian (Fig. 4). Two offsets were needed to match the observed experimental spectra: a shift by 9 eV and the addition of a background cross-section of 38 cm^2/g for the lower orbitals. Peak locations were reliably reproduced across the spectrum. Relative amplitudes were in good agreement in the near-edge region but failed to reproduce the peak amplitudes further away from the edge.

We also convolved the data with a 10 and 20 eV Lorentzian. This improved agreement with the extended region peaks but at the expense of the near-edge peaks. The experimental energy band width at the beamline used by Chantler et al. (2001) is only 2.2 eV at 9 keV across this energy range (Chantler et al., 2004). Clearly some energy dependent broadening is not accounted for in the model.

An obvious cause is thermal vibrations of atoms about their mean lattice sites. This results in differing path lengths for different absorbing atoms or equivalently for different X-ray absorption events of the same absorbing atom. This yields an energy dependent dampening of the oscillations, which increases with energy above the edge. It has been reported that thermal effects in the near-edge region are negligible (Rehr and Albers, 2000; Dimakis and Bunker, 1998), and as such have been ignored in the FDMNES code. As we extend the FDMNES program into the XAFS region it becomes apparent that the thermal effects can no longer be ignored, and appear to be significant by the *second* peak. Similar results have been seen in silver (Cosgriff et al., 2005).

A uniform broadening is *inadequate* to explain the data. Since *additional broadening* at the edge is indicated, thermal broadening appears inadequate as a sole explanation of the experimental data.

5. Conclusion

The FDMNES method is useful and relevant not just in the near-edge region but also in the extended region. Peak locations are reliably reproduced. Further investigations into thermal and other broadening processes are required to accurately reproduce peak amplitudes. Although computationally intensive, this method could lead to an examination of the interstitial potential that cannot be achieved with cluster methods reliant on the muffin-tin potential.

Acknowledgements

The authors acknowledge Prof. Y. Joly, Lucas F. Smale, Zwi Barnea and the experimental team, as well as funding from the ASRP and ARC.

References

Aberdam, D., 2001. European Synchrotron Research Facility (unpublished).

Chantler, C.T., 1994. Towards improved form factor tables. In: Materlik, G., Sparks, C.J., Fischer, K. (Eds.), Resonant Anomalous X-Ray Scattering—Theory and Applications. North-Holland, Amsterdam.

Chantler, C.T., 2000. Detailed tabulation of atomic form factors, photoelectric absorption and scattering cross section, and mass attenuation coefficients in the vicinity of absorption edges in the soft X-ray ($Z = 30$–36, $Z = 60$–89, $E = 0.1$–10 keV), addressing convergence issues of earlier work. J. Phys. Chem. Ref. Data 29 (4), 597–1056.

Chantler, C.T., Tran, C.Q., Barnea, Z., Paterson, D., Cookson, D.J., Balaic, D.X., 2001. Measurement of the X-ray mass attenuation coefficient of copper using 8.85–20 keV synchrotron radiation. Phys. Rev. A 64(6), 062506/1-15.

Chantler, C.T., Tran, C.Q., Cookson, D.J., 2004. Precise measurement of the lattice spacing of LaB_6 standard powder by the X-ray extended range technique using synchrotron radiation. Phys. Rev. A 69 (4), 42101.

Cosgriff, E.C., Chantler, C.T., Witte, C., Smale, L.F., Tran, C.Q., 2005. Atomic cluster-structure calculation of the X-ray near-edge absorption of silver. Phys. Lett. A, in press.

Dimakis, N., Bunker, G., 1998. Ab initio single- and multiple-scattering EXAFS Debye–Waller factors: Raman and infrared data. Phys. Rev. B 58 (5), 2467–2475.

Joly, Y., 1996. Finite-difference method for the calculation of low-energy positron diffraction. Phys. Rev. B 53 (19), 13029–13037.

Joly, Y., 2001. X-ray absorption near-edge structure calculations beyond the muffin-tin approximation. Phys. Rev. B 63 (12), 125120.

McGuire, E.J., 1970. K-shell Auger transition rates and fluorescence yields for elements Ar–Xe. Phys. Rev. A 2 (2), 273–278.

Rehr, J.J., Albers, R.C., 2000. Theoretical approaches to X-ray absorption fine structure. Rev. Mod. Phys. 72 (3), 621–654.

Scofield, J.H., 1974. Relativistic Hartree–Slater values for K and L X-ray emission rates. At. Data Nucl. Data Tables 14 (2), 121–137.

Tran, C.Q., Chantler, C.T., Barnea, Z., de Jonge, M.D., Dhal, B.B., Chung, C.T.Y., Paterson, D., Wang, J., 2005. Measurement of the X-ray mass attenuation coefficient of silver using the X-ray-extended range technique. J. Phys. B 38 (1), 89–107.

Wong, J., 1999. Reference X-ray Spectra of Metal Foils, EXAFS Materials, Inc., 871 El Cerro Blvd, Danville, CA.